Validation of ICESat-2 Derived Data Products on Freshwater Lakes: Bathymetry, Diffuse Attenuation Coefficient for Downwelling Irradiance (K_d), and Particulate Backscatter Coefficient (b_{bp})

Ray H. Watkins, Michael J. Sayers, Robert A. Shuchman, *Member, IEEE*, and Karl R. Bosse

***Abstract*— Monitoring large bodies of water, such as the Laurentian Great Lakes in North America, can be challenging and costly. The bathymetry, the diffuse attenuation coefficient for downwelling irradiance (K_d), and the particulate backscattering coefficient (b_{bp}) are important metrics in monitoring water quality in lakes and have typically been measured in two ways: 1) via in situ sampling campaigns, which are expensive, time-consuming, and have a low spatial resolution; and 2) via passive optical imagery, which can have errors in excess of 50%. Recently, Ice, Cloud, and land Elevation Satellite-2 (ICESAT-2), an active light detection and ranging (LiDAR)-based satellite, has proven effective in deriving the bathymetry, K_d, and b_{bp} in the global oceans. However, validation of such metrics has never been done on satellite flyovers taken on the same day as in situ measurements. Likewise, studies on freshwater environments have been limited. Here, we compare in situ data sampled from Lake Michigan and Big Glen Lake between August 13th and 14th, 2021, and results derived from an ICESat-2 flyover in the same region on August 14th, 2021. We find excellent agreement between the in situ values and the satellite-derived values for all three metrics. This suggests that ICESat-2 and other future LiDAR-based satellites will be powerful tools for monitoring large freshwater lakes.**

***Index Terms*— Bathymetry, diffuse attenuation coefficient for downwelling irradiance (K_d), Ice, Cloud, and land Elevation Satellite-2 (ICESAT-2), Laurentian Great Lakes, light detection and ranging (LiDAR), particulate backscattering coefficient (b_{bp}).**

I. Introduction

ICESAT-2 was launched by the National Aeronautics and Space Administration (NASA) in 2018 with the primary goals of measuring changes in polar ice sheets, measuring the free-board amount of sea ice, and measuring the amount of vegetation canopy across Earth [1]. This is done with the onboard ATLAS LiDAR, which uses green (532 nm) light to map photon returns across six beams, resulting in 70 cm along profile resolution [2]. Since its launch in 2018, secondary uses of Ice, Cloud, and land Elevation Satellite-2 (ICESAT-2) capabilities have been assessed and implemented. To start, the bathymetry of both shallow coastal seaways [3] and water greater than 25 m has been recorded [4], with results typically validated by and combined with optical imagery and in situ values to produce high resolution gridded bathymetry [5].

Along with bathymetry, by building upon work done with previous spaceborne LiDAR-based systems [6], [7], recent studies have shown optical properties can be derived from ICESat-2 photon return. Both the diffuse attenuation coefficient for downwelling irradiance (K_d) and the particulate backscattering coefficient (b_{bp}) can be obtained from the distribution of photons in the water column [8]. b_{bp} is a central inherent optical property that gives important insight into ecological processes that happen in large bodies of water. On the global oceans, b_{bp} has been used to quantify global carbon stocks [9], track the vertical migrations of ocean animals [10], and quantify primary production [11]. Likewise, K_d is critical for understanding how much light is penetrating a given water column (i.e., photic zone depth), which has been shown to control biochemical and physical processes such as primary production that dictate the abundance of life within a water column [12].

Most studies calculating ICESat-2 bathymetry and all studies calculating ICESat-2 optical properties have been done on the global oceans. However, ICESat-2 still makes passes over some of the world's largest lakes, including Lake Michigan. Nearshore bathymetry is important in the scope of the Laurentian Great Lakes as changes due to lake warming can affect the spawning environments of fish and can also change local boating patterns [13]. Likewise, decreases in K_d and b_{bp} over a 14 year period on Lake Michigan and Lake Huron have been tied to the effect of dreissenid mussels, phosphorus abatement, and climate change on the lakes [14].

Here, we perform two experiments with respect to ICESat-2. To start, we evaluate for the first time measurements of bathymetry, K_d, and b_{bp} calculated from ICESat-2 to in situ values sampled at the same time and location as the satellite flyover. This is done in two separate locations: a large freshwater lake (Lake Michigan) and a small freshwater lake (Big Glen Lake) in the area surrounding Glen Arbor, Michigan, USA. This test serves to validate the reliability of ICESat-2-derived products to ground truth measurements and can

Manuscript received 12 October 2022; revised 3 March 2023; accepted 21 March 2023. Date of publication 24 March 2023; date of current version 7 April 2023. This work was supported in part by the Great Lakes Restoration Initiative [between Environmental Protection Agency (EPA) and National Oceanic and Atmospheric Administration (NOAA)] under Agreement DW-013-92543701 and in part by the Cooperative Institute for Great Lakes Research (CIGLR) through the NOAA Cooperative Agreement with the University of Michigan (CIGLR contribution number is 1205) under Grant NA17OAR4320152. *(Corresponding author: Ray H. Watkins.)*

The authors are with the Michigan Tech Research Institute, Michigan Technological University, Ann Arbor, MI 48104 USA (e-mail: rhwatkin@mtu.edu).

Digital Object Identifier 10.1109/LGRS.2023.3261551

be taken as an expansion of past studies in other locations. Second, we appraise the value of spaceborne LiDAR remote sensing as a tool to monitor large, freshwater lakes. We close by commenting on the role that spaceborne LiDAR can play in the future of Great Lakes remote sensing.

II. Data and Methods

A. In Situ Sampling

Our sampling campaign took place on Lake Michigan and Big Glen Lake in the northwest region of Michigan, USA, as indicated by Fig. 1. Sampling was done in two stages: First, bathymetry data were collected on both lakes via a boat survey using a sonar depth sounder. This was done along the projected path of the ICESat-2 flyover. Lake conditions resulted in a slight horizontal offset between the in situ sampling profile and the ICESat-2 profile, especially on Big Glen Lake. Bathymetric data sampling took place the day prior to the flyover on August 13th, 2021. Optical property sampling on Big Glen Lake also took place on August 13th. Optical property data on Lake Michigan were sampled at approximately the same time as the August 14th, 2021 ICESat-2 flyover, which occurred at ≈3 : 30 P.M. EST.

K_d was measured using a Seabird Hyperpro II profiling radiometer following previously reported methods [15]. Briefly, the profiler was cast in a free-fall to a geometric depth corresponding to two optical depths at 490 nm, approximately 20 m in Lake Michigan and 13 m in Big Glen Lake. Ten casts were made at each site to reduce the effects of wave focusing in the upper water column. Spectral downwelling plane irradiance (E_d) profiles (10) were binned (mean) at 0.5 m depth intervals. Spectral K_d of the first optical depth (depth at which 10% of the light just below the surface remains [16]) was computed from the binned profiles by calculating a linear fit of the log-transformed E_d profile (from 0 m to 1 optical depth) where the slope of the fit is taken as K_d (m^{-1}).

b_{bp} was computed for nine spectral bands (410, 440, 490, 510, 532, 667, 705, 715) using a Seabird ECO BB-9 scattering meter attached to a profiling frame that also included a Seabird AC-S and CTD. Vertical profiles were made through the photic zone at each site, as estimated from the profiling radiometer. Profiles of b_{bp} were averaged into 0.5 m bins. A Secchi disk was also deployed at each sampling location, as a crude estimation of optical depth is needed for K_d and b_{bp} calculations from ICESat-2.

B. ICESat-2 Bathymetry, K_d and b_{bp}

ATLAS/ICESat-2 L2A Global Geolocated Photon Data was used to derive all products. This data set contains the coordinates and elevations of all photons that are returned to ICESat-2 [17]. Specifically, we use data from the middle, a strong beam of a flyover on Lake Michigan and Big Glen Lake from August 14th, 2021, shown in Fig 1. Bathymetry was calculated from the photon returns following the procedure in [18]. Here, an empirical calculation is used to group bottom returns from a satellite in high, medium, and low confidence readings of the bathymetry. These readings are then corrected

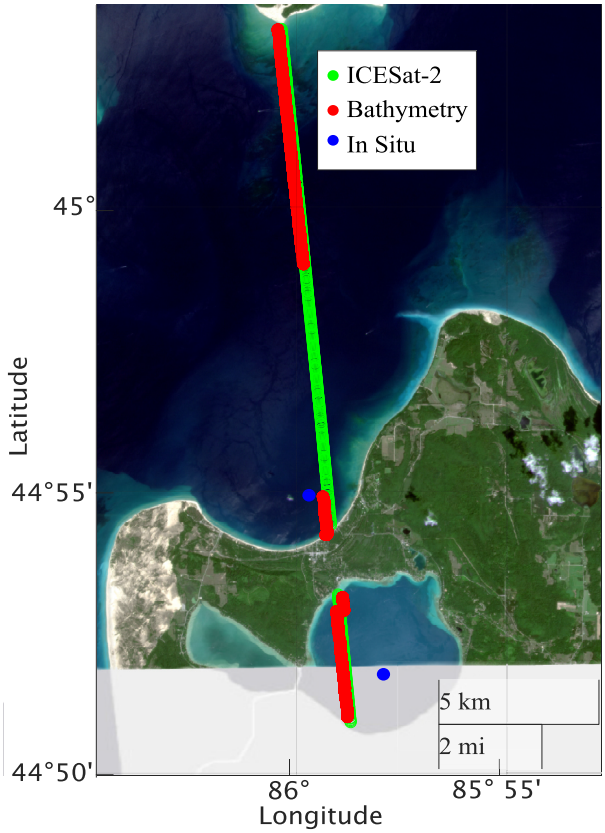

Fig. 1. Sampling location on Lake Michigan and Big Glen Lake. The red line indicates the location of the in situ bathymetric sampling. The blue dots show the location of the optical property in situ sampling. Finally, the green line shows the location of the ICESat-2 flyover. Overlain is the PlanetScope Ortho image of Glen Arbor, MI, USA taken on August 14th, 2021 showing the conditions on Lake Michigan and Big Glen Lake during the ICESat-2 flyover used in this survey. Note the stark difference in water color between Lake Michigan and Big Glen Lake.

for refraction that occurs as the photons move through the water [19]. In this study, we only evaluate the high-confidence bathymetry returns.

Both K_d and b_{bp} are calculated using the method developed by [8], [20]. For the scope of this study, both K_d and b_{bp} refer to the metrics sampled at a wavelength of 532 nm. Here, the photons along the flight line of the satellite are grouped into 0.001 degree latitude by 0.1 m bins on each body of water. These bins are then normalized and averaged over the length of the flight track to create a photon distribution at depth for each lake. Deconvolution of the signal is performed to remove the effects of potential after pulses that occur as the LiDAR signal passes through the water/surface interface.

K_d is then taken as the slope of the decay of the photon signal through the water column between 3 m and 1.5 optical depths, where the limits represent data limitations due to after pulses and LiDAR penetration depth respectively. The optical depths are estimated from Secchi disk measurements and are taken as 12 m in Lake Michigan and 4 m in Big Glen Lake. Column integrated b_{bp} and depth-dependent b_{bp} are calculated directly from the binned, normalized, photon return using predetermined constants and dynamic variables in the derivation. For the scope of our study, we assumed the backscatter of freshwater (B_w) to be 0.005 m^{-1} [21] and the

wind speed (v) to be 7 m * s^{-1} (measured in situ). All other inputs as well as an in-depth analysis of these calculations can be found in [8].

III. Results

A. Bathymetry Validation

We first examined how ICESat-2 derived bathymetry compared to in situ sampled bathymetry at the same relative time (within 24 h) and the same location. This was done across Big Glen Lake, shown in Fig. 2(a), and Lake Michigan, shown in Fig. 2(b). To start, we looked at the results from Big Glen Lake and found a somewhat substantial horizontal offset between the in situ sampled data and the satellite-derived data, resulting in a medium difference of 1.22 m. This offset was caused by differences in the sampling line and the satellite line, with the overall trend in the bathymetry being similar between the two sources of data. On Lake Michigan, Fig. 2(b), the in situ sampling line was much closer to the satellite line, resulting in a medium percent difference of only 0.67 m between the two.

Our results from the bathymetry survey also showed the maximum depth that ICESat-2 could reliably sense on freshwater lakes. On Big Glen Lake, the maximum sensed depth from ICESat-2 was ~8 m while on Lake Michigan, the satellite sensed depth was ~12 m. In each location, a Secchi disk was deployed, with results yielding 3.2 m on Big Glen Lake and 12 m on Lake Michigan. Therefore, the maximum depth is largely dependent on the clarity of the water, with increasing clarity (Secchi disk depth) related to larger maximum depth, an occurrence previously noted in other water environments [19].

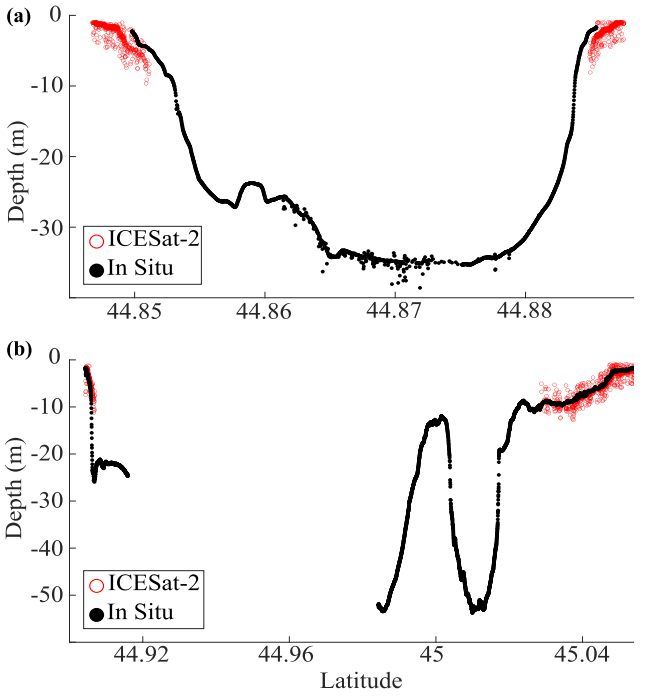

Fig. 2. Comparison between (black) in situ sampled values and (red) ICESat-2 derived values. (a) Big Glen Lake. (b) Lake Michigan. Outliers in in situ sampling values are due to errors in sampling and are not true trends in the data.

B. K_d and b_{bp} Validation

We next examined how in situ sampled K_d and b_{bp} values compared to values derived from ICESat-2. To start, we look at our results on Big Glen Lake and find that for K_d, the in situ value (0.156 m^{-1}) agreed very well with the satellite-derived value (0.158 m^{-1}), with a percent difference of only 1.27% between them. K_d is derived from the slope of the blue line shown in Fig. 3(a). On Lake Michigan, shown in Fig. 3(b), we also found that the in situ sampled K_d (0.0996 m^{-1}) agreed very well with the ICESat-2 K_d (0.0921 m^{-1}), with a percent difference of only 7.82%. Our results for K_d are also consistent with our maximum depth results from our bathymetry survey, with the clearer lake (Lake Michigan) having a lower K_d value than Big Glen Lake. Likewise, our K_d results agree with Secchi disk measurements, where the Secchi depth was much smaller for Big Glen Lake than for Lake Michigan.

We also compared satellite derived b_{bp} to in situ sampled b_{bp} on Lake Michigan, shown by Fig. 3(b). This was done by looking at the photon distribution at depth, and then the column integrating the result. The photons used to calculate b_{bp} are taken from around 3 m below the surface, down to 1.5 optical depths below the surface (18 m), as indicated by the red points in Fig. 3(b). Our results once again show great coherence between the in situ values (0.0046 m^{-1}) and the satellite values (0.00463 m^{-1}), with a percent difference of only 0.65%. Unfortunately, we were unable to sample b_{bp} on Big Glen Lake due to limitations of deploying our device on the day of the Big Glen Lake data collection. However, we were still able to derive b_{bp} on Big Glen Lake, which is shown by Fig. 3(a). Here, the value of column integrated b_{bp} was 0.0110 m^{-1}. Though there is no direct compassion to an in situ value, this b_{bp} is consistent with studies that indicate that increasing K_d should yield increasing b_{bp} [22].

C. b_{bp} at Depth

Our final analysis compared b_{bp} sampled at a depth between in situ value and ICESat-2 derived values on Lake Michigan, which is indicated by Fig. 4(a). Here, b_{bp} is compared at 1 m intervals ranging from 3 m to 1.5 optical depths, which is taken to be 18 m on Lake Michigan. We found a satellite-derived b_{bp} at a depth that is much more variable than in situ values. The standard deviation at depth for ICESat-2 b_{bp} is 0.0023 m^{-1} while the standard deviation for in situ values is 0.0002 m^{-1}, an order of magnitude less. Likewise, the in situ b_{bp} is mostly constant at depth while the ICESat-2 b_{bp} is elevated close to the surface of the water, decays to a minimum of 0.0012 m^{-1} at around 10 m of depth, and then spikes to a maximum value at the bottom of the profile greater than 0.015 m^{-1}. Also shown in Fig. 4(b) is the total chlorophyll concentration in sampled at depth and the water temperature, both sampled at the same time and location as the in situ values in Fig. 4(a). Note that the water temperature is mostly constant below 5 m, indicating that all data shown was collected above the thermocline.

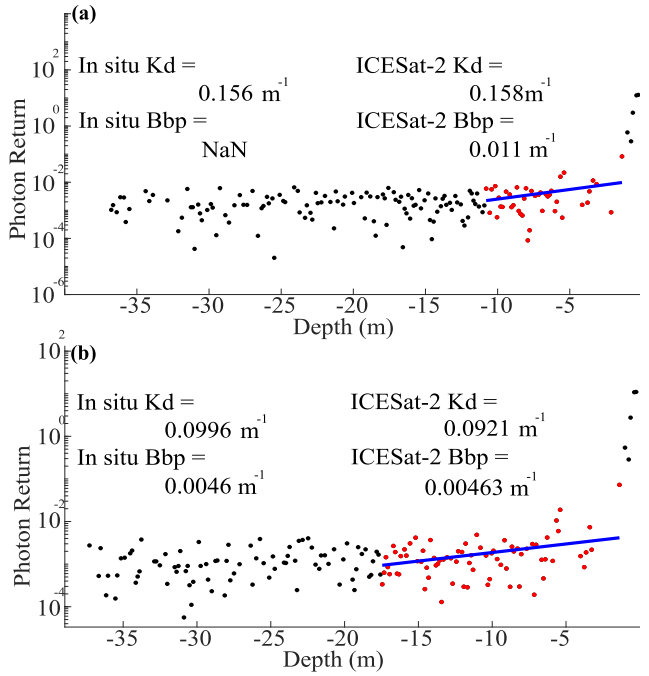

Fig. 3. K_d and b_{bp} comparison between in situ sampled values and ICESat-2 derived values on (a) Big Glen Lake and (b) Lake Michigan. The black dots in each figure represent the binned photons while the reds represent the binned photons used in the calculations. The blue line represents the fit slope in calculating K_d.

IV. Discussion

Here, for the first time, we compare a variety of ICESat-2 derived metrics regarding the subsurface properties of freshwater to the same metrics sampled in situ within the same day of each other. To start, we looked at the bathymetry on two separate lakes with different levels of water clarity and found that ICESat-2 was an effective tool for measuring mid-depth bathymetry. Specifically, ICESat-2 was able to measure the bathymetry effectively down to approximately one optical depth, which is variable between lakes based on the water clarity at the given location. The depth limit likely partially stems from only taking the high-confidence bathymetry photons. If medium and low confidence signals are considered, this would likely increase the range of depths that are able to be observed by ICESat-2, but would also likely increase errors.

In the study, we also examined the effectiveness of monitoring K_d on large, freshwater lakes using ICESat-2. We found that in two different lakes with differing optical properties, ICESat-2 derived K_d values agreed almost perfectly with in situ sampled values. This was also verified empirically by comparing Secci disk depths between the two locations. Likewise, in looking at the contrast in watercolor in the optical satellite imagery, we can also draw an empirical conclusion that both bodies of water should have substantially different values of K_d (Fig. 1). While K_d was only sampled at one location for ICESat-2, by taking an average value over a segment of the flyover K_d can also be derived at every point along every satellite flyover on Lake Michigan. This could effectively map and monitor how K_d changes in different locations on the lake. Likewise, there are approximately six

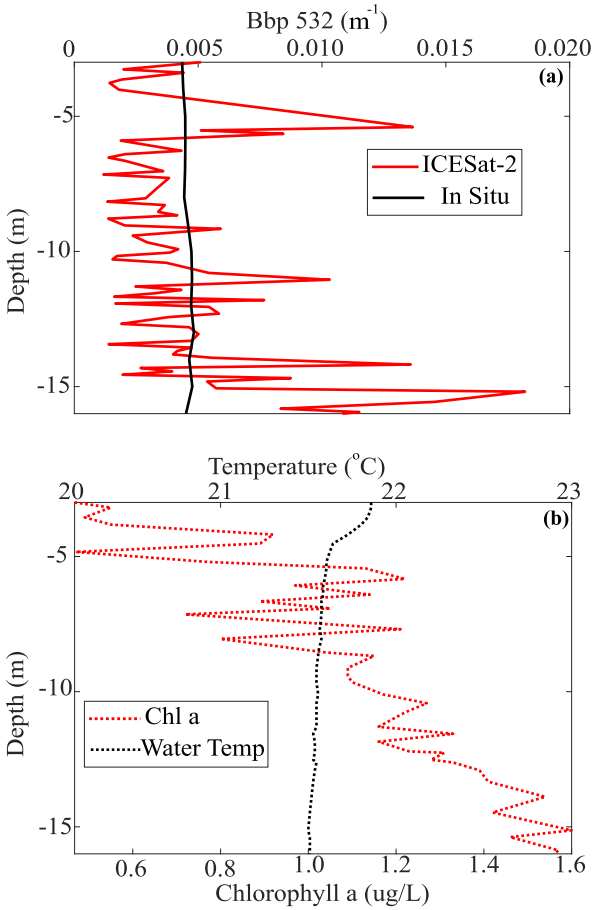

Fig. 4. (a) b_{bp} sampled at depth for (red) ICESat-2 and (black) in situ values. (b) Chlorophyll a (red dotted) and water temperature (black dotted) in situ sampled values at the same location/time as those in (a).

separate flyovers (depending on the quality of the data return) in varying locations on Lake Michigan every month, which would allow for monitoring of K_d on the lake on a monthly basis.

The final subsurface metric that was monitored using ICESat-2 on the freshwater lakes in our survey was b_{bp}. This was done as a column-integrated value of Lake Michigan and Big Glen Lake, and also calculated as a function of depth on Lake Michigan. On Lake Michigan, where in situ b_{bp} was also sampled, the column integrated b_{bp} from ICESat-2 was again nearly identical to the in situ sampled value. For the b_{bp} at depth, ICESat-2 was able to effectively sample b_{bp} between 3 and 18 m (1.5 optical depths). Compared to the in situ values at the depth, the ICESat-2 results were much more variable. This is likely related to taking an average across a 10 km long satellite track as opposed to sampling at one particular location. However, trends in the ICESat-2 derived b_{bp} (Fig. 4(a)) seem to correlate with trends in Chlorophyll a concentration where both metrics increase as a function of depth. That said, further sampling and analysis are needed to validate any connections between the two. Finally, as with K_d, b_{bp} could also be sampled across all of Lake Michigan on a monthly basis, which is likely where the applicability of these results lies. Here, the structure of the water column (in regards to b_{bp}) between 3 and 18 m could also be mapped, which would be novel for a large, freshwater lake.

V. Conclusion

We report that ICESat-2 will be a valuable tool in the future for monitoring and remote sensing of not only Lake Michigan, but also other large, freshwater, bodies of water. A comparison between in situ values and satellite-derived values of bathymetry, K_d, and b_{bp} all show good coherence. We note that more sampling campaigns are likely needed for a more thorough evaluation of the metrics, especially for nighttime flyovers of ICESat-2, which were not evaluated in this study. However, the preliminary results from this survey certainly point toward the incorporation of ICESat-2 into the remote sensing toolbox on the Great Lakes and beyond.

Acknowledgment

The authors would like to thank the journal editors and reviewer. They would also like to thank NOAA and EPA for providing financial support. Specifically, they would like to thank Dr. Hinchey and Dr. Tuchman from Great Lakes National Program Office (GLNPO) and Ruberg and Vander Woude from NOAA/Great Lakes Environmental Research Laboratory (GLERL) for encouraging this assessment.

References

[1] A. J. Martino, T. A. Neumann, N. T. Kurtz, and D. McLennan, "ICESat-2 mission overview and early performance," in *Proc. SPIE*, Oct. 2019, pp. 68–77, doi: 10.1117/12.2534938.

[2] A. Neuenschwander and K. Pitts, "The ATL08 land and vegetation product for the ICESat-2 mission," *Remote Sens. Environ.*, vol. 221, pp. 247–259, Feb. 2019, doi: 10.1016/j.rse.2018.11.005.

[3] H.-J. Hsu et al., "A semi-empirical scheme for bathymetric mapping in shallow water by ICESat-2 and Sentinel-2: A case study in the South China Sea," *ISPRS J. Photogramm. Remote Sens.*, vol. 178, pp. 1–19, Aug. 2021.

[4] Y. Ma et al., "Satellite-derived bathymetry using the ICESat-2 LiDAR and Sentinel-2 imagery datasets," *Remote Sens. Environ.*, vol. 250, Dec. 2020, Art. no. 112047, doi: 10.1016/j.rse.2020.112047.

[5] Y. Li, H. Gao, M. F. Jasinski, S. Zhang, and J. D. Stoll, "Deriving high-resolution reservoir bathymetry from ICESat-2 prototype photon-counting LiDAR and Landsat imagery," *IEEE Trans. Geosci. Remote Sens.*, vol. 57, no. 10, pp. 7883–7893, Oct. 2019, doi: 10.1109/TGRS.2019.2917012.

[6] M. J. Behrenfeld et al., "Annual boom–bust cycles of polar phytoplankton biomass revealed by space-based LiDAR," *Nature Geosci.*, vol. 10, no. 2, pp. 118–122, Dec. 2016, doi: 10.1038/ngeo2861.

[7] X. Lu, Y. Hu, C. Trepte, S. Zeng, and J. H. Churnside, "Ocean subsurface studies with the CALIPSO spaceborne LiDAR," *J. Geophys. Res., Oceans*, vol. 119, no. 7, pp. 4305–4317, Jul. 2014, doi: 10.1002/2014jc009970.

[8] X. Lu, Y. Hu, Y. Yang, P. Bontempi, A. Omar, and R. Baize, "Antarctic spring ice-edge blooms observed from space by ICESat-2," *Remote Sens. Environ.*, vol. 245, Aug. 2020, Art. no. 111827, doi: 10.1016/j.rse.2020.111827.

[9] V. Martinez-Vicente, G. Dall'Olmo, G. Tarran, E. Boss, and S. Sathyendranath, "Optical backscattering is correlated with phytoplankton carbon across the Atlantic Ocean," *Geophys. Res. Lett.*, vol. 40, no. 6, pp. 1154–1158, Mar. 2013, doi: 10.1002/grl.50252.

[10] M. J. Behrenfeld et al., "Global satellite-observed daily vertical migrations of ocean animals," *Nature*, vol. 576, no. 7786, pp. 257–261, Nov. 2019, doi: 10.1038/s41586-019-1796-9.

[11] J. A. Schulien, M. J. Behrenfeld, J. W. Hair, C. A. Hostetler, and M. S. Twardowski, "Vertically-resolved phytoplankton carbon and net primary production from a high spectral resolution LiDAR," *Opt. Exp.*, vol. 25, no. 12, p. 13577, Jun. 2017, doi: 10.1364/oe.25.013577.

[12] Z.-P. Lee, "Diffuse attenuation coefficient of downwelling irradiance: An evaluation of remote sensing methods," *J. Geophys. Res.*, vol. 110, no. C2, pp. 1–9, 2005, doi: 10.1029/2004jc002573.

[13] Y. Zhong, M. Notaro, and S. J. Vavrus, "Spatially variable warming of the Laurentian Great Lakes: An interaction of bathymetry and climate," *Climate Dyn.*, vol. 52, nos. 9–10, pp. 5833–5848, Oct. 2018, doi: 10.1007/s00382-018-4481-z.

[14] F. Yousef, R. Shuchman, M. Sayers, G. Fahnenstiel, and A. Henareh, "Water clarity of the Upper Great Lakes: Tracking changes between 1998–2012," *J. Great Lakes Res.*, vol. 43, no. 2, pp. 239–247, Apr. 2017, doi: 10.1016/j.jglr.2016.12.002.

[15] M. J. Sayers et al., "Spatial and temporal variability of inherent and apparent optical properties in western Lake Erie: Implications for water quality remote sensing," *J. Great Lakes Res.*, vol. 45, no. 3, pp. 490–507, Jun. 2019, doi: 10.1016/j.jglr.2019.03.011.

[16] H. R. Gordon and W. R. McCluney, "Estimation of the depth of sunlight penetration in the sea for remote sensing," *Appl. Opt.*, vol. 14, no. 2, p. 413, Feb. 1975, doi: 10.1364/ao.14.000413.

[17] T. A. Neumann et al. (2021). *ATLAS/ICESat-2 L2A Global Geolocated Photon Data, Version 5*. [Online]. Available: http://nsidc.org/data/atl03/versions/5

[18] H. Ranndal, P. Sigaard Christiansen, P. Kliving, O. Baltazar Andersen, and K. Nielsen, "Evaluation of a statistical approach for extracting shallow water bathymetry signals from ICESat-2 ATL03 photon data," *Remote Sens.*, vol. 13, no. 17, p. 3548, Sep. 2021, doi: 10.3390/rs13173548.

[19] C. E. Parrish, L. A. Magruder, A. L. Neuenschwander, N. Forfinski-Sarkozi, M. Alonzo, and M. Jasinski, "Validation of ICESat-2 ATLAS bathymetry and analysis of ATLAS's bathymetric mapping performance," *Remote Sens.*, vol. 11, no. 14, p. 1634, Jul. 2019, doi: 10.3390/rs11141634.

[20] X. Lu et al., "New ocean subsurface optical properties from space LiDARs: CALIOP/CALIPSO and ATLAS/ICESat-2," *Earth Space Sci.*, vol. 8, no. 10, Oct. 2021, Art. no. e2021EA001839, doi: 10.1029/2021ea001839.

[21] G. Thursby, S. Rego, and D. Keith, "Data report for calibration of a bio-optical model for Narragansett Bay," U.S. Environ. Protection Agency, Washington, DC, USA, Tech. Rep. EPA/600/R-15/211, 2015.

[22] S. P. Tiwari and P. Shanmugam, "An optical model for deriving the spectral particulate backscattering coefficients in oceanic waters," *Ocean Sci.*, vol. 9, no. 6, pp. 987–1001, Nov. 2013, doi: 10.5194/os-9-987-2013.